# Multi-Objective Optimization of Ocean Thermal Energy Conversion Power Plant via Genetic Algorithm

Alireza Najafi
*B. Sc. Student*
*Mechanical Engineering Faculty*
*K. N. Toosi University of Technology*
*Tehran, Iran*
Email: alireza.najafi88@gmail.com

Shahab Rezaee
*B. Sc. Student*
*Mechanical Engineering Faculty*
*K. N. Toosi University of Technology*
*Tehran, Iran*
Email: shahabrezaee@gmail.com

Farschad Torabi
*Assistant Professor*
*Mechanical Engineering Faculty*
*K. N. Toosi University of Technology*
*Tehran, Iran*
Email: ftorabi@kntu.ac.ir

***Abstract*—Design of an ocean thermal energy conversion (OTEC) power plant needs a local thermal condition evaluation, in order to satisfy the constructional limits as well as economical considerations. In this paper, performance of 10 MW, 50 MW, and 100 MW OTEC power plants in locations with surface water temperature between 22 $^\circ$C to 28 $^\circ$C has been investigated and the optimum set of design parameters has been presented. For this approach, a multi-objective optimization via genetic algorithm is carried out. A set of optimal solutions, called Pareto front, for each inlet warm sea water temperature is obtained. Inlet warm sea water velocity and pipe diameter as well as cold sea water, and condenser and evaporator temperatures have been considered as optimization parameters to minimize the total pumping power and heat transfer area as objectives.**

***Index Terms*—OTEC, Multi-objective, Genetic algorithm, optimization, Pareto front**

## NOMENCLATURE

| | |
|---|---|
| $A$ | Heat transfer surface area $(\mathrm{m}^2)$ |
| $C_\mathrm{p}$ | Specific heat at constant pressure $(\mathrm{kJ\,kg^{-1}K^{-1}})$ |
| $d$ | Pipe diameter $(\mathrm{m})$ |
| $D$ | Diameter $(\mathrm{m})$ |
| $f$ | Coefficient of friction |
| g | Acceleration of gravity $(\mathrm{m\,s^{-2}})$ |
| $h$ | Enthalpy $(\mathrm{kJ\,kg^{-1}})$ |
| $\Delta H$ | Pressure loss $(\mathrm{kPa})$ |
| $k$ | Heat conductivity $(\mathrm{W\,m^{-1}K^{-1}})$ |
| $l$ | Length $(\mathrm{m})$ |
| $L$ | Latent heat $(\mathrm{kJ\,kg^{-1}})$ |
| $\dot{m}$ | Mass flow rate $(\mathrm{kg\,s^{-1}})$ |
| $p$ | Pressure $(\mathrm{Pa})$ |
| $P$ | Power $(\mathrm{W})$ |
| $Q$ | Heat flow rate $(\mathrm{kJ})$ |
| $Re$ | Reynolds number |
| $T$ | Temperature $(^\circ\mathrm{C})$ |
| $\Delta T_\mathrm{m}$ | Logarithmic mean temperature difference $(^\circ\mathrm{C})$ |
| $U$ | Overall heat-transfer coefficient $(\mathrm{W\,m^{-2}K^{-1}})$ |
| $V$ | Velocity $(\mathrm{m\,s^{-1}})$ |
| $w$ | Width of plate $(\mathrm{m})$ |
| $\Delta y$ | Clearance $(\mathrm{m})$ |

Greek symbols

| | |
|---|---|
| $\delta$ | Thickness $(\mathrm{m})$ |
| $\eta$ | Efficiency |
| $\rho$ | Density $(\mathrm{kg\,m^{-3}})$ |
| $\lambda$ | Friction factor |
| $\mu$ | Dynamic viscosity $(\mathrm{Pa.s})$ |
| $\nu$ | Kinematic viscosity $(\mathrm{m^2\,s^{-1}})$ |

Subscripts

| | |
|---|---|
| C | Condenser |
| CS | Cold sea water |
| d | Density |
| eq | Equivalent |
| E | Evaporator |
| G | Generator |
| I | Input |
| N | Net |
| O | Output |
| P | Piping, Pump |
| T | Total, Turbine |
| W | Wall |
| WF | Working fluid |
| WS | Warm sea water |

## I. INTRODUCTION

Demand for energy has been rising quickly due to the economic development and population growth all over the world. Currently, a considerable portion of this energy comes from fossil fuels. However, an increasing worldwide concern about the impermanence of these sources and the harmful effects of fossil fuels on the environment augmented the social interest in using renewable energies. Among these sources, ocean thermal energy conversion (OTEC) is a power generation method which utilizes the temperature difference between warm surface water and cold deep water of the oceans to produce electricity. Therefore, OTEC is a reliable source of energy in islands near equator and also oil platforms owing to the capability of generating rather stable amount of electricity during the year and in all hours.

Since D'Arsonoval conceived the OTEC concept in 1881, and Claude first implemented the data and idea in 1930, there has been a wide range of interest in OTEC technology [1]. Depending on the cycles used, different types of OTEC systems have been proposed using open cycle, closed cycle or hybrid cycle configurations. At the present, only closed-cycle OTEC can achieve economic feasibility compared with other two OTEC configurations. A closed cycle OTEC uses high vapor density liquids such as freon, propane or ammonia as its working fluid, unlike the open-cycle OTEC which utilizes seawater, instead [2].

Due to a small temperature difference (approximately 15 - 25 °C) between the surface water and deep water of the ocean, the Rankine-cycle efficiency is limited to be about 3% - 5%. Therefore, there has been considerable research effort aimed at improving the performance of an OTEC power plant. The effect of various working fluids on the performance of a cycle has been investigated by Kim et al. [3]. They also examined the influence of different cycles such as closed system, a regeneration system, and a Kalina system on improving the efficiency. Furthermore, there are other works dedicated to increase the efficiency of an OTEC closed cycle by some combinations. For instance, Yamada et al. [4] proposed a solar-boosted OTEC system and stated that the net thermal efficiency of the operation with 20 °C solar boost is 2.7 times higher than that of OTEC operation under the daytime conditions at Kumejima Island. A combination of OTEC cycle with solar pond was introduced by Straatman et al. [5] to increase the temperature difference in the Rankine cycle, which leads to an improved efficiency of 12%.

Since the heat exchanger cost (about 25 - 50 percent of the plant cost) is one of the major costs of the OTEC plant, lots of efforts have been made to find the best heat exchanger types and configurations. Nakaoka and Uehara [6], [7] conducted experiments to test the performance of an OTEC system with shell-and-plate-type evaporator and condenser.

From an economic point of view, difference between OTEC power plants and other source of energies such as fossil fuels and nuclear energy have been discussed by Odum which utilized a method called "Emergy Evaluation Method" (emergy spelled with an 'm') [8]. Horazak and Rabas [9] also developed a model based on minimizing the whole OTEC system components which can be economically attractive. It is stated that the capital cost optimization of an entire power system results in a lower system cost than does the optimization of individual components.

Optimizing the OTEC plant performance is another approach that lead to system efficiency increase. Yeh et al. [10] theoretically investigated the effects of the temperature and flow rate of cold seawater on the net output of an OTEC plant. They conducted a sensitivity analysis by changing just one variable at a time. Another approach to reach this goal was by the specific power analysis [11], [12]. Wu utilized a finite-time thermodynamic approach to a Rankine closed cycle OTEC analysis which gave a much more realistic heat engine power, specific power and efficiency prediction than did the classical Carnot ideal cycle. Furthermore, a detailed optimization was carried out by Uehara and Ikegami [13] using Powell method.

In real world it is rare for any problem to concern only a single objective. In most of engineering problems, objectives are in conflict with each other, the fact that makes optimization with respect to a single objective to yield inappropriate results with respect to other objectives. As an example, most of the optimization works mentioned previously, only considered one objective function. However, reasonable solution to a multi-objective problem is to investigate a set of solutions, each of which satisfies the objectives at an acceptable level without being dominated by any other solution [14]. Evolutionary algorithms, like genetic algorithm, owing to their special characteristics, has been used for multi-objective optimization during recent years.

In the present work a multi-objective optimization with the net output power and construction cost as objective functions is conducted. By searching through different effective parameters, a set of optimal designs and configurations is presented.

## II. System Model

Aside from the media used to accomplish the heat transfer, a closed cycle OTEC is the same as a Rankine cycle. The medium gains the heat through an evaporator from the ocean surface warm water, and produces power by passing through a turbine. Cold water from deep parts of the ocean cools the outlet flow from the turbine in a condenser and completes the cycle as shown in Fig. 1. The temperature-entropy (T-s) diagram of a closed Rankine cycle used in OTEC power plants is illustrated in Fig. 2.

Heat transfer between pipes and sea water is assumed to be negligible, due to the massive amount of water flow rates and the large pipe diameters. Therefore, the temperature change of inlet cold sea water is not taken into account [13], [10].

The net power $P_{\mathrm{N}}$ of the OTEC operation is written as [13]

$$P_{\mathrm{N}} = P_{\mathrm{G}} - P_{\mathrm{TP}} \tag{1}$$

where $P_{\mathrm{G}}$ is the turbine generator power and $P_{\mathrm{TP}}$ is the total pumping power in a power plant defined as:

$$P_{\mathrm{TP}} = P_{\mathrm{WS}} + P_{\mathrm{CS}} + P_{\mathrm{WF}} \tag{2}$$

$P_{\mathrm{WS}}$, $P_{\mathrm{CS}}$, and $P_{\mathrm{WF}}$ are the pumping powers required for warm sea water, cold sea water, and the working fluid, respectively. The value of turbine generator power, $P_{\mathrm{G}}$ is calculated from the product of the mass flow rate of the

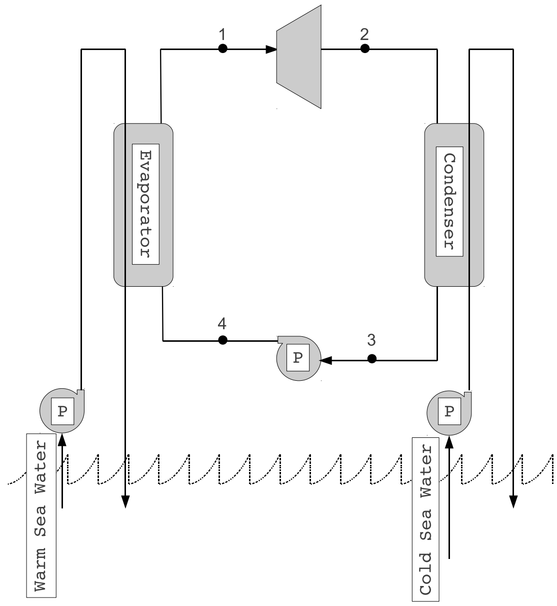


Fig. 1. Schematics of conventional closed Rankine cycle OTEC operation

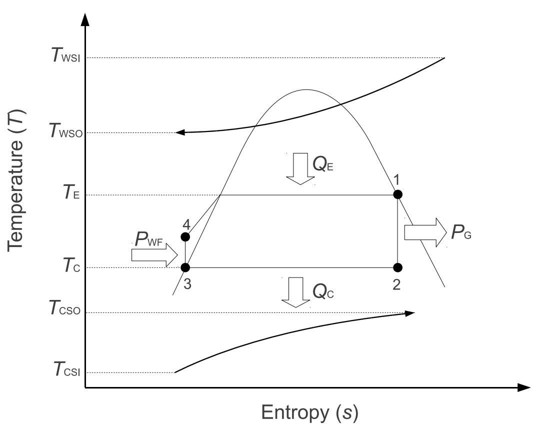


Fig. 2. T-s diagram of the closed Rankine cycle

working-fluid and the adiabatic enthalpy difference between the evaporator and the condenser as:

$$P_{\mathrm{G}} = \dot{m}_{\mathrm{WF}}\eta_{\mathrm{T}}\eta_{\mathrm{G}}\left(h_1 - h_2\right) \tag{3}$$

where $\eta_{\mathrm{T}}$ and $\eta_{\mathrm{G}}$ are the turbine and generator efficiencies, respectively. Other power parameters shown in Eq. (2) are given as:

$$P_{\mathrm{WS}} = \dot{m}_{\mathrm{WS}}\Delta H_{\mathrm{WS}}\mathrm{g}/\eta_{\mathrm{WSP}} \tag{4}$$

$$P_{\mathrm{CS}} = \dot{m}_{\mathrm{CS}}\Delta H_{\mathrm{CS}}\mathrm{g}/\eta_{\mathrm{CSP}} \tag{5}$$

$$P_{\mathrm{WF}} = \dot{m}_{\mathrm{WF}}\Delta H_{\mathrm{WF}}\mathrm{g}/\eta_{\mathrm{WFP}} \tag{6}$$

where g is the acceleration due to gravity and $\dot{m}_{\mathrm{WS}}$, $\dot{m}_{\mathrm{CS}}$, $\dot{m}_{\mathrm{WF}}$, $\Delta H_{\mathrm{WS}}$, $\Delta H_{\mathrm{CS}}$, $\Delta H_{\mathrm{WF}}$, $\eta_{\mathrm{WSP}}$, $\eta_{\mathrm{CSP}}$, and $\eta_{\mathrm{WFP}}$ are mass flow rates, total pressure differences (i.e. head), and pump efficiencies of the piping used for warm sea water, cold sea water, and working fluid, respectively.

$\Delta H_{\mathrm{CS}}$ is the total pressure difference of the cold sea water pipe, defined as:

$$\Delta H_{\mathrm{CS}} = \left(\Delta H_{\mathrm{CS}}\right)_{\mathrm{P}} + \left(\Delta H_{\mathrm{CS}}\right)_{\mathrm{C}} + \left(\Delta H_{\mathrm{CS}}\right)_{\mathrm{d}} \tag{7}$$

where $\left(\Delta H_{\mathrm{CS}}\right)_{\mathrm{P}}$ is the friction factor of the cold sea water straight pipe, defined as [13]:

$$\left(\Delta H_{\mathrm{CS}}\right)_{\mathrm{P}} = 6.82\frac{l_{\mathrm{CS}}}{{d_{\mathrm{CS}}}^{1.17}}\left(\frac{V_{\mathrm{CS}}}{C_{\mathrm{CS}}}\right)^{1.85} \tag{8}$$

$$C_{\mathrm{CS}} = 100 \tag{9}$$

where $l_{\mathrm{CS}}$ is the length of the cold sea water pipe, $d_{\mathrm{CS}}$ is the diameter of the cold sea water pipe, and $V_{\mathrm{CS}}$ is the velocity of the cold sea water. $\left(\Delta H_{\mathrm{CS}}\right)_{\mathrm{C}}$ is the cold sea water pressure difference in the condenser defined as:

$$\left(\Delta H_{\mathrm{CS}}\right)_{\mathrm{C}} = \lambda_{\mathrm{C}}\frac{{V_{\mathrm{CS}}}^2}{2\mathrm{g}}\frac{l_{\mathrm{C}}}{\left(D_{\mathrm{eq}}\right)_{\mathrm{C}}} \tag{10}$$

$l_{\mathrm{C}}$ is the length of the condenser plate and $D_{\mathrm{eq}}$ is the equivalent diameter and is equal to $2\Delta y$ [6]. The value of $\lambda_{\mathrm{C}}$ is taken from Uehara et al. [15].

$\left(\Delta H_{\mathrm{CS}}\right)_d$ is the pressure difference caused by the density difference between the warm and the cold sea water, defined as:

$$\left(\Delta H_{\mathrm{CS}}\right)_d = l_{\mathrm{CS}} - \frac{1}{\rho_{\mathrm{CS}}}\left(\frac{1}{2}\left(\rho_{\mathrm{WS}} + \rho_{\mathrm{CS}}\right)l_{\mathrm{CS}}\right) \tag{11}$$

$\Delta H_{\mathrm{WS}}$ is also the total pressure difference of the warm sea water pipe, defined as:

$$\Delta H_{\mathrm{WS}} = \left(\Delta H_{\mathrm{WS}}\right)_{\mathrm{P}} + \left(\Delta H_{\mathrm{WS}}\right)_{\mathrm{E}} \tag{12}$$

where the the values of $\left(\Delta H_{\mathrm{WS}}\right)_P$ and $\left(\Delta H_{\mathrm{WS}}\right)_{\mathrm{E}}$ are evaluated the same as the cold sea water pipe calculation with warm water pipe properties.

$\Delta H_{\mathrm{WF}}$ is the total pressure difference of the working fluid piping, defined as:

$$\Delta H_{\mathrm{WF}} = \left(\Delta H_{\mathrm{WF}}\right)_{\Delta p} + \left(\Delta H_{\mathrm{WF}}\right)_{\mathrm{P}} + \left(\Delta H_{\mathrm{WF}}\right)_{\mathrm{C}} \tag{13}$$

$\left(\Delta H_{\mathrm{WF}}\right)_{\Delta p}$ is the saturation pressure difference between evaporator and condenser, defined as:

$$\left(\Delta H_{\mathrm{WF}}\right)_{\Delta p} = \frac{p_{\mathrm{E}} - p_{\mathrm{C}}}{\rho\mathrm{g}} \tag{14}$$

where $\rho$ is the density of the working fluid. $\left(\Delta H_{\mathrm{WF}}\right)_{\mathrm{C}}$ is the pressure difference on the working fluid side in the condenser and is given as:

$$\left(\Delta H_{\mathrm{WF}}\right)_{\mathrm{C}} = 6.19\times 10^6 \mathrm{Re_V}^{-1.21}\frac{V_{\mathrm{C}}^2}{2\mathrm{g}}\frac{l_{\mathrm{C}}}{\left(D_{\mathrm{eq}}\right)_{\mathrm{C}}} \tag{15}$$

$$\mathrm{Re}_{\mathrm{V}} = \frac{V_{\mathrm{C}} l_{\mathrm{C}}}{\nu_{\mathrm{C}}} \tag{16}$$

where $V_{\mathrm{C}}$ is the velocity of the working fluid in the condenser, $l_{\mathrm{C}}$ is the length of the condenser plate and $(D_{\mathrm{eq}})$ is the equivalent diameter of the condenser plate.

The total heat transfer surface area, $A_{\mathrm{T}}$, is given as:

$$A_{\mathrm{T}} = A_{\mathrm{E}} + A_{\mathrm{C}} \tag{17}$$

$A_{\mathrm{E}}$ and $A_{\mathrm{C}}$ are the heat transfer areas of the evaporator and the condenser which are shell and plate type heat exchangers and defined as:

$$A_{\mathrm{E}} = \frac{Q_{\mathrm{E}}}{U_{\mathrm{E}}(\Delta T_{\mathrm{m}})_{\mathrm{E}}} = \frac{\dot{m}_{\mathrm{WS}} C_{P_{\mathrm{WS}}} (T_{\mathrm{WSI}} - T_{\mathrm{WSO}})}{U_{\mathrm{E}}(\Delta T_{\mathrm{m}})_{\mathrm{E}}} \tag{18}$$

$$A_{\mathrm{C}} = \frac{Q_{\mathrm{C}}}{U_{\mathrm{C}}(\Delta T_{\mathrm{m}})_{\mathrm{C}}} = \frac{\dot{m}_{\mathrm{CS}} C_{P_{\mathrm{CS}}} (T_{\mathrm{CSI}} - T_{\mathrm{CSO}})}{U_{\mathrm{C}}(\Delta T_{\mathrm{m}})_{\mathrm{C}}} \tag{19}$$

where $(\Delta T_{\mathrm{m}})_{\mathrm{E}}$ and $(\Delta T_{\mathrm{m}})_{\mathrm{C}}$ are also logarithmic mean temperature differences of the evaporator and the condenser, respectively, defined as:

$$(\Delta T_{\mathrm{m}})_{\mathrm{E}} = \frac{(T_{\mathrm{WSI}} - T_{\mathrm{E}}) - (T_{\mathrm{WSO}} - T_{\mathrm{E}})}{\ln\left(\frac{(T_{\mathrm{WSI}} - T_{\mathrm{E}})}{(T_{\mathrm{WSO}} - T_{\mathrm{E}})}\right)} \tag{20}$$

$$(\Delta T_{\mathrm{m}})_{\mathrm{C}} = \frac{(T_{\mathrm{C}} - T_{\mathrm{CSI}}) - (T_{\mathrm{C}} - T_{\mathrm{CSO}})}{\ln\left(\frac{(T_{\mathrm{C}} - T_{\mathrm{CSI}})}{(T_{\mathrm{C}} - T_{\mathrm{CSO}})}\right)} \tag{21}$$

$Q_{\mathrm{E}}$ and $Q_{\mathrm{C}}$ are also the heat transfer rate of the evaporator and the condenser, respectively, defined as:

$$Q_{\mathrm{E}} = \dot{m}_{\mathrm{WF}} (h_1 - h_4) \tag{22}$$

$$Q_{\mathrm{C}} = \dot{m}_{\mathrm{WF}} (h_2 - h_3) \tag{23}$$

where $\dot{m}_{\mathrm{WF}}$ is the working fluid flow rate, given as:

$$\dot{m}_{\mathrm{WF}} = \frac{P_G}{\eta_{\mathrm{T}} \eta_G (h_1 - h_2)} \tag{24}$$

## III. Optimization

### A. GENETIC ALGORITHM

The genetic algorithm (GA) is a method for solving both constrained and unconstrained optimization problems that is based on natural selection, the process that drives biological evolution [16]. The GA can be applied to solve a variety of optimization problems that are not well suited for standard optimization algorithms, including problems in which the objective function is discontinuous, nondifferentiable, stochastic, or highly nonlinear. Trapping in a local minimum or maximum, while there is a better answer somewhere else, is a problem which most of the normal optimization methods suffer. However, GA has multiple adjustment options such as mutation ratio which intentionally deflects the convergance path to ascertain the locating of the best answer. Moreover, GA searches more thorough in defined bounds than other search methods in less time consuming process. These characteristics make GA a suitable method for utilizing in this paper.

### B. MULTI-OBJECTIVE OPTIMIZATION

Multi-objective optimization is concerned with the minimization of a vector of objectives F(x) that can be the subject of a number of constraints or bounds [16]:

$$\begin{aligned}&\min / \max F(x) = [f_1(x), f_2(x), ..., f_n(x)]\\ &x_l \leq x \leq x_u\end{aligned}$$

Since $F(x)$ is a vector, if any of the components of $F(x)$ are competing, there is no unique solution to this problem. Instead, the concept of noninferiority (also called Pareto optimality) must be used to characterize the objectives. A noninferior solution, also called Pareto optima, is one in which an improvement in one objective requires a degradation of another. A general goal in multi-objective optimization is constructing the Pareto optima, by which one can find the best set of optimal answers for a defined problem. In a Pareto graph, solutions cannot be improved with respect to any objective without worsening at least one other objective. Therefore, with respect to the application utilized, a trade-off between choosing an optimal solution must be made or in general purposes the solution with the least distance from the intersection of the axes might be chosen.

### C. OBJECTIVES AND CONSTRAINTS

In the present work, the total pumping power and heat transfer area of an OTEC power plant are considered as objective functions. For this goal, inlet warm sea water velocity and pipe diameter as well as cold sea water temperature, and condenser and evaporator temperatures have been considered as optimization parameters. These simulations are carried out in different fixed inlet warm sea water temperatures. Desired solution is one with the least heat transfer area and total pumping power.

In this section, various inequality constraints are written to define the feasible region for the optimization problem, as well as feasible operating conditions for an optimal performance. Limitations for the water velocity and diameter of cold and warm sea water pipes are

$$0.7 \leq V_{\mathrm{CS}}, V_{\mathrm{WS}} \leq 2 \tag{25}$$

$$0 \leq d_{\mathrm{CS}}, d_{\mathrm{WS}} \leq 25 \tag{26}$$

Condenser and evaporator working temperatures are constant and the limitations for their values are

$$T_{\mathrm{WSI}} - 7 \leq T_{\mathrm{E}} \leq T_{\mathrm{WSI}} - 3 \tag{27}$$

$$T_{\mathrm{CSI}} + 3 \leq T_{\mathrm{C}} \leq T_{\mathrm{CSI}} + 7 \tag{28}$$

where $T_{\mathrm{CSI}}$ is the inlet cold sea water from the 1000 m deep, which is set 4 °C constantly.

## IV. Results and Discussion

To validate the mathematical model, the results from the simulations are compared with a case study from Uehara and Ikegami [13] in TABLE I. It can be observed that the results are in an acceptable agreement with different inlet warm sea water temperatures.

TABLE I
VALIDATION

| | $T_{\mathrm{WSI}}$ (°C) | $P_{\mathrm{N}}$ (MW) | $P_{\mathrm{WS}}$ (MW) | $P_{\mathrm{CS}}$ (MW) | $P_{\mathrm{WF}}$ (MW) |
|---|---|---|---|---|---|
| Ref. [13] | 28 | 71.4 | 11.1 | 15.6 | 1.97 |
| Present work | 28 | 71.8 | 12.1 | 14.4 | 1.42 |

The optimization result consists of three parts for 100 MW, 50 MW and 10 MW OTEC power plants. Final Pareto optimal set generated by multi-objective genetic algorithm is depicted in figures 3 to 5. Optimization was terminated due to the fact that average change in value of the spread of Pareto set over specified limitations. Some of the optimum derived values for optimization parameters are given in TABLE II.

It can be observed that aside from the power range of the plants, heat transfer required area will decrease as the input warm sea water temperature increases in the same pumping power value. The construction cost of the plant, which mainly depends on the heat exchangers size, also decreases as a result of reducing the heat transfer area. Therefore, the cost of an OTEC plant will be less in locations with higher surface water temperature with the same pumping power or the performance of a plant will be better in mentioned locations with the same configuration. For instance, in a 100 MW power plant with the total pumping power of 14 MW, heat transfer area in 28 °C will be one fifth of the amount in 22 °C.

The effect of higher input warm water temperature can also be noticed from the Pareto fronts in figures 3 to 5. The best set of data in a Pareto front is a set with lower distance from the intersection of the axes. Therefore, the set of resultant data from 28 °C which has the minimum distance from the axes intersection is the best set in all different OTEC plants.

From the data in TABLE II, it can be understood that in locations with surface water temperature of 22 °C, construction of a 100 MW OTEC power plant may be infeasible due to the extremely high pipe diameter values which intensifies construction costs and problems. In these locations a smaller plant could be more practical. In either case a boosting cycles such as solar–boosted OTEC could be employed to increase the input warm water temperature to an acceptable diameter range.

In the optimization method performed by Uehara and Ikegami [13], the pumping power value in 28 °C was calculated as about 30 MW while in the present work by utilizing GA the mentioned value reduced to half, which results in higher total net power of the plant.

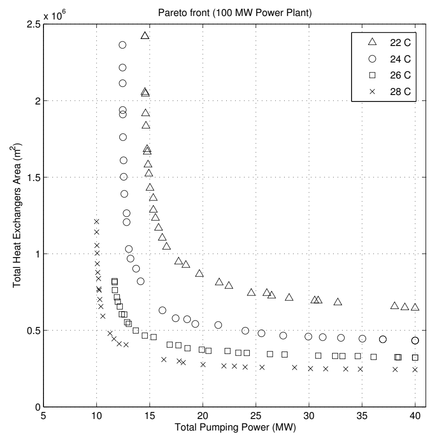


Fig. 3. Derived Pareto front for a 100 MW power plant

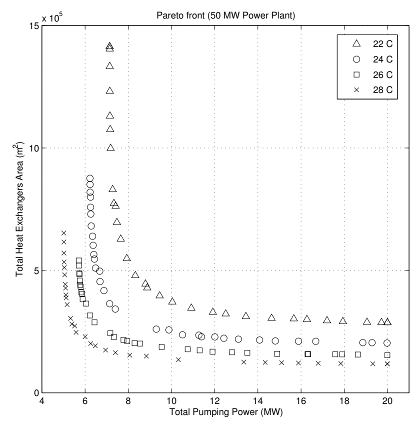


Fig. 4. Derived Pareto front for a 50 MW power plant

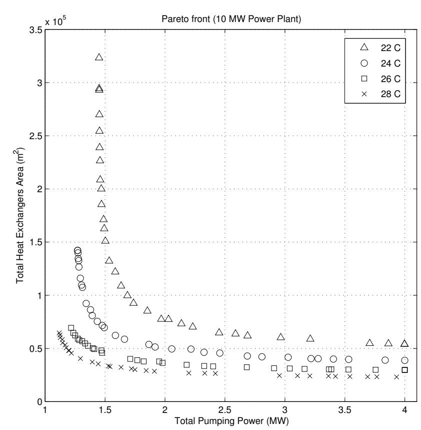


Fig. 5. Derived Pareto front for a 10 MW power plant

TABLE II
SOME OF OPTIMUM VALUES OF OPTIMIZATION PARAMETERS

| | 100 MW | | | | | | | | 50 MW | | | | | | | |
|---|---|---|---|---|---|---|---|---|---|---|---|---|---|---|---|---|
| $T_{\mathrm{WSI}}$ (°C) | $d_{\mathrm{WS}}$ (m) | $V_{\mathrm{WS}}$ (m/s) | $T_{\mathrm{E}}$ (°C) | $d_{\mathrm{CS}}$ (m) | $V_{\mathrm{CS}}$ (m/s) | $T_{\mathrm{C}}$ (°C) | $P_{\mathrm{TP}}$ (MW) | $A_{\mathrm{T}}$ $\left(\mathrm{m} \times 10^5\right)$ | $d_{\mathrm{WS}}$ (m) | $V_{\mathrm{WS}}$ (m/s) | $T_{\mathrm{E}}$ (°C) | $d_{\mathrm{CS}}$ (m) | $V_{\mathrm{CS}}$ (m/s) | $T_{\mathrm{C}}$ (°C) | $P_{\mathrm{TP}}$ (MW) | $A_{\mathrm{T}}$ $\left(\mathrm{m} \times 10^5\right)$ |
| 22 | 20.34 | 0.702 | 17.34 | 18.723 | 0.718 | 9.06 | 14.562 | 24.82 | 14.305 | 0.7 | 17.623 | 13.276 | 0.707 | 8.8 | 7.144 | 14.897 |
| | 20.712 | 0.751 | 17.39 | 19.662 | 0.916 | 8.79 | 22.733 | 9.066 | 20.712 | 0.751 | 17.39 | 19.662 | 0.916 | 8.79 | 22.733 | 9.066 |
| | 22.82 | 0.816 | 17.39 | 19.486 | 0.981 | 8.71 | 29.454 | 7.226 | 19.309 | 0.766 | 17.46 | 15.714 | 0.785 | 8.59 | 14.044 | 3.254 |
| | 23.929 | 0.865 | 17.47 | 19.954 | 1.04 | 8.74 | 36.737 | 6.605 | 19.893 | 0.788 | 17.32 | 18.267 | 0.88 | 8.43 | 19.721 | 2.871 |
| 24 | 18.812 | 0.7 | 19.55 | 16.417 | 0.712 | 9.5 | 12.441 | 26.482 | 12.716 | 0.706 | 19.045 | 12.188 | 0.701 | 9.13 | 6.244 | 8.77 |
| | 19.01 | 0.704 | 19.34 | 16.439 | 0.842 | 9.46 | 15.143 | 8.927 | 13.871 | 0.709 | 19.03 | 12.692 | 0.704 | 9.05 | 7.04 | 3.927 |
| | 24.329 | 0.746 | 19.23 | 19.084 | 0.914 | 9.41 | 25.525 | 4.804 | 14.39 | 0.75 | 18.88 | 17.147 | 0.758 | 9.06 | 11.612 | 2.515 |
| | 24.688 | 0.809 | 19.11 | 19.745 | 1.081 | 9.35 | 36.957 | 4.411 | 18.023 | 0.792 | 18.81 | 17.973 | 0.849 | 8.93 | 17.786 | 2.077 |
| 26 | 17.176 | 0.701 | 20.59 | 16.141 | 0.703 | 9.16 | 11.719 | 8.256 | 12.692 | 0.708 | 21.769 | 10.616 | 0.701 | 9.49 | 5.772 | 6.331 |
| | 18.739 | 0.706 | 20.54 | 16.86 | 0.847 | 9.29 | 16.201 | 4.568 | 13.653 | 0.713 | 21.63 | 12.051 | 0.783 | 9.61 | 7.754 | 2.426 |
| | 22.042 | 0.763 | 20.52 | 18.729 | 0.922 | 9.33 | 24.857 | 3.567 | 17.804 | 0.769 | 21.23 | 12.519 | 0.798 | 9.57 | 11.636 | 1.843 |
| | 22.898 | 0.808 | 20.5 | 19.209 | 1.077 | 9.58 | 34.599 | 3.315 | 17.796 | 0.802 | 20.92 | 16.879 | 0.858 | 9.69 | 17.581 | 1.572 |
| 28 | 15.858 | 0.701 | 23.057 | 13.968 | 0.7 | 10.11 | 10.035 | 12.155 | 11.237 | 0.701 | 22.688 | 9.652 | 0.713 | 10.74 | 5.017 | 7.326 |
| | 16.146 | 0.703 | 23.02 | 18.06 | 0.737 | 10.11 | 14.122 | 4.974 | 11.272 | 0.828 | 22.77 | 9.566 | 0.759 | 10.73 | 6.578 | 2.732 |
| | 21.737 | 0.733 | 22.36 | 22.188 | 0.746 | 10.08 | 22.975 | 2.66 | 17.341 | 0.77 | 22.66 | 10.394 | 0.744 | 10.42 | 9.745 | 1.756 |
| | 23.374 | 0.851 | 22.35 | 23.61 | 0.843 | 10.06 | 35.769 | 2.464 | 18.215 | 0.754 | 22.21 | 19.274 | 0.779 | 10.23 | 17.959 | 1.197 |

## V. CONCLUSION

A multi-objective optimization via genetic algorithm was carried out in order to find the best performance of an OTEC power plant which had the least heat transfer area, simultaneously. Effect of power plant locations with different surface water temperature in 22 °C, 24 °C, 26 °C, and 28 °C has been also considered. It was shown that in locations with higher surface water temperature, less heat transfer area is needed which results in less heat exchangers constructional cost. Results from the present work optimization showed a performance improvement in comparison with the similar works in the literature. It is also observed that in 100 MW power plants in locations with lower warm inlet water temperatures, larger pipe diameters is needed that might be infeasible in some cases due to higher pipeline construction costs and problems. However, it is recommended to boost the cycles with solar power to increase the efficiency of the plant.


## ACKNOWLEDGMENT

The authors gratefully acknowledge the support of Department of Energy Systems of K. N. Toosi University of Technology.


## REFERENCES


[1] W. H. Avery and C. Wu, *Renewable Energy from the Ocean: A Guide to OTEC*. Oxford University Press, 1994.

[2] C. Xie, S. Wang, L. Zhang, and S. J. Hu, "Improvement of proton exchange membrane fuel cell overall efficiency by integrating heat to electricity conversion," *Power Sources*, vol. 191, pp. 433–441, 2009.

[3] N. J. Kim, K. C. Ng, and W. Chun, "Using the condenser effluent from a nuclear power plant for ocean thermal energy conversion (otec)," *International Communications in Heat and Mass Transfer*, vol. 36, pp. 1008–1013, 2009.

[4] N. Yamada, A. Hoshi, and Y. Ikegami, "Performance simulation of solar boosted ocean thermal energy conversion plant," *Renewable Energy*, vol. 34, pp. 1752–1758, 2009.

[5] P. J. Straatman and W. G. van Sark, "A new hybrid ocean thermal energy conversion offshore solar pond (otec osp) design a cost optimization approach," *Solar Energy*, vol. 82, pp. 520–527, 2008.

[6] T. Nakaoka and H. Uehara, "Performance test of a shell and plate type evaporator for otec," *Experimental Thermal and Fluid Science*, pp. 283–291, 1988.

[7] ——, "Performance test of a shell and plate type condenser for otec," *Experimental Thermal and Fluid Science*, pp. 275–281, 1988.

[8] H. T. Odum, "Emergy evaluation of an otec electrical power system," *Energy*, vol. 25, pp. 389–393, 2000.

[9] D. A. Horazak and T. J. . Rabas, "Capital cost system optimization of otec power modules," *Energy Resources Technology*, vol. 101, pp. 74–79, 1979.

[10] R. H. Yeh, T. Z. Su, and M. S. Yang, "Maximum output of an otec power plant," *Ocean Engineering*, vol. 32, pp. 685–700, 2005.

[11] C. Wu, "Specific power optimization of closed cycle otec plants," *Ocean Engng*, vol. 17, pp. 307–314, 1990.

[12] ——, "Specific power analysis of thermoelectric otec plants," *Ocean Engng*, vol. 20, pp. 433–442, 1993.

[13] H. Uehara and Y. Ikegami, "Optimization of a closed-cycle otec system," *Solar Energy Engineering*, vol. 112, pp. 247–256, 1990.

[14] A. Konak, D. Coit, and A. Smith, "Multi-objective optimization using genetic algorithm: A tutorial," *Reliability Engineering and System Safety*, vol. 91, pp. 992–1007, 2006.

[15] H. Uehara, H. Kusuda, M. Monde, T. Nakaoka, and H. Sumitomo, "Shell-and-plate-type heat exchangers for otec plants," *Solar Energy Enigeering*, vol. 106, pp. 286–290, 2011.

[16] *Genetic Algorithm and Direct Search ToolboxTM User's Guide*, Version 2.3 (release 2008a) ed., March 2008.